Resolving the Rise and Fall of Star Formation in Galaxies
Proceedings IAU Symposium No. 373, 2023
T. Wong & W.-T. Kim, eds.
doi:10.1017/S1743921322003854

The cold gas supply through cosmic time: insights on the galaxy assembly at early epochs

Manuel Aravena

Núcleo de Astronomía, Facultad de Ingeniería y Ciencias,
Universidad Diego Portales, 8370191 Santiago, Chile
email: manuel.aravenaa@mail.udp.cl

Abstract.

Remarkable progress has been made in the last few years in understanding the global properties of galaxies and how they evolve through cosmic time. Major focus has been given to studies of how the availability of molecular gas regulates star-forming activity and galaxy growth, the eventual quenching of star formation, and how these mechanisms evolve through cosmic time. Most of these advances have been made thanks to ALMA and the upgraded capabilities of NOEMA. In this contribution, I briey review the latest constraints on the molecular gas content based on dierent tracers of the interstellar medium (ISM; dust continuum and CO, [CI] and [CII] line emission), including recent determinations of the molecular gas fraction, gas depletion timescales, and molecular gas cosmic density provided by the recent ALMA programs out to $z \sim 7$. Finally, I concentrate on recent and ongoing studies aiming to spatially and kinematically resolve the cold ISM and star formation activity down to kpc scales in galaxies out to $z \sim 6-7$, which represent an unprecedented view of the galaxy assembly and feedback processes in the early universe.

Keywords. galaxies: high-redshift, galaxies: evolution, galaxies: ISM

1. Rise and fall of star formation in galaxies

One of the main results of galaxy evolution in the past decades has been the determination of the cosmic star formation rate (SFR) density of the universe out to redshifts of 10 (Madau & Dickinson 2014). Three main epochs are defined, including an epoch where the first galaxies appeared and the star formation steadily increased ($z > 6$), an epoch of galaxy assembly where most of the stars in the universe were formed($1 < z < 4$), and the epoch of galaxy quenching ($z < 1$).

A key result has been the determination that most star-forming galaxies appear to form a tight relation between the SFRs and their stellar masses at all redshifts. The galaxies in this so-called "main sequence" appear to have the predominant contribution to the cosmic SFR density (e.g. Elbaz et al. 2007). Understanding what drives this evolution and how galaxies build up their stellar mass (as a function of their location in the SFR vs. stellar mass plane) is among the most fundamental question in galaxy evolution studies. To describe the physical processes involved in the galaxy's growth, it is critical to measure their cold interstellar medium (ISM) molecular gas content, as it represents the fuel through which stars form.

2. Measuring the molecular ISM in distant galaxies

Several methods have been used to measure the molecular gas mass in high-redshift galaxies. These include measurements of the continuum and line emission from the rest-frame far-infrared and submillimeter regimes.

2.1. *Dust continuum emission*

This is the most commonly used method to measure the molecular gas mass regarding the number of sources targeted. Two approaches have been used.

The first one requires the acquisition of photometry of the target galaxy through the full infrared regime, with at least three data points, enabling to conduct spectral energy distribution (SED) fitting with standard routines, or simply approximating the dust SED as a multi-component gray body spectrum. Various physical parameters can be obtained, including the dust temperature, mass, emissivity index, and size. Using the dust mass and assuming a dust-to-gas mass ratio (typically $\sim 20-100$ for galaxies with close to solar metallicities), an estimate of the molecular gas mass can be obtained. The main caveat is that it can be particularly observationally expensive to target statistical samples of sources as this method needs observations in several far-infrared and submillimeter bands. Furthermore, obtaining photometry in the far-infrared regime, at wavelengths shorter than 350μm is almost prohibited from the ground, requiring space observatories, which are currently lacking after decommissioning *Spitzer* and *Herschel*.

The second approach corresponds to a simplified version, in which an estimate of the dust mass can be obtained from a single far-infrared data point in the Rayleigh-Jeans (RJ) limit. This method has received particular interest since it is easier to detect observationally and benefits from a negative K-correction out to high redshifts (e.g. Scoville et al. 2014). This method essentially uses the fact that the dust emission in the RJ regime ($> 200\mu$m) is most sensitive to the dust mass. This method has been calibrated for massive star-forming galaxies and has been widely used to measure dust and molecular gas masses in large samples of galaxies as it requires a single photometric data point at relatively long wavelengths (typically 850μm or 1.2mm). The main disadvantage of this method is that it is not clear that it would apply to galaxies with conditions like low stellar masses or metallicities and further calibrations are needed.

2.2. *CO, [CI] and [CI] line emission*

The method to measure the molecular gas mass through cold molecular gas tracers like the CO and [CI] lines is among the most traditional methods. This approach assumes that these tracers are directly linked to the bulk of molecular gas, H_2, and relies on the assumption of a line luminosity to gas mass conversion factor α. The latter has been observed to vary through different environments and metallicity (Bolatto et al. 2013). For starburst and "normal" galaxies typically values of ~ 1 and 4.6 $M_\odot$ [K km s^{-1} pc^2]$^{-1}$ are assumed.

The main advantage of this method is that line emission can provide significantly more information on dynamics, particularly estimates of the dynamical mass of the system. Similarly to the full dust SED method, it is more observationally expensive than simply observing a single continuum data point. For CO line emission, the observation of higher rotational transitions is less sensitive to the total molecular gas mass. It thus has the additional requirement of assuming line ratios to convert the emission into the lower J CO transitions.

The [CII] has recently been proposed as an estimator of the molecular gas mass. The [CII] line emission arises from various environments (neutral, ionized, photodissociation

https://doi.org/10.1017/S1743921322003854 Published online by Cambridge University Press

regions in molecular clouds). Thus its emission has been calibrated to measure the amount of neutral (HI) and molecular gas (H_2) mass (Heintz et al. 2021; Zanella et al. 2018). As with the CO and [CI] line emission, the [CII] molecular gas mass estimates require the assumption of a (calibrated) conversion factor between the [CII] line luminosity. Based on the Zanella et al. results, $\alpha_{[CII]} \sim 30\ M_\odot\ L^{-1}$. While it is under debate whether the [CII] method is applicable in different contexts, the main advantage is to enable access to a higher redshift regime not accessible to CO and/or dust emission due to their general faintness, and large cosmological distances, as [CII] is the among the brightest far-infrared emission lines in galaxies.

3. ISM surveys of star-forming galaxies at high redshift

3.1. *Targeted surveys of the ISM at high redshift*

Submillimeter galaxies. Significant efforts have been devoted in the last 20+ years to conducting blank-field sub-millimeter surveys over large sky areas with bolometer cameras in single-dish telescopes (e.g. Smail et al. 1997; Hughes et al. 1998). These surveys discovered an important population of dust-rich starburst galaxies at high redshift that contributed a significant fraction of the cosmic SFR density (e.g. Casey et al. 2014).

Given their selection wavelength, by construction, every (sub)millimeter continuum survey traces the cold dust content out to $z < 3$, and similarly for surveys at 1.2mm out to $z \sim 6$. However, detailed studies of this population have only been enabled through the identification of multiwavelength counterparts through interferometric (sub)millimeter follow-up with facilities like the ALMA, NOEMA, and the SMA. Despite the significant improvement in our understanding of the physical properties of SMGs in the last decade, only a few dedicated surveys have been performed to measure the molecular gas content in CO line emission for both unlensed (Bothwell et al. 2013; Sharon et al. 2016; Wardlow et al. 2018; Birkin et al. 2021) and lensed samples (Aravena et al. 2016; Harrington et al. 2018; Yang et al. 2017; Cañ ameras et al. 2018).

Main sequence galaxies and starbursts. Since these (sub)millimeter surveys are only able to grasp the brightest dusty star-forming galaxies in the sky, pinpointing the typical population of galaxies at $z \sim 1-3$, with SFRs $\sim 50-200\ M_\odot\ yr^{-1}$, has required targeted observations of dust continuum and molecular gas (CO and [CI]) emission in galaxies that have been pre-selected through their optical colors and/or faint IR emission detected in *Herschel* IR surveys (e.g. Tacconi et al. 2020; Valentino et al. 2018).

Quiescent galaxies. The advent of sensitive ALMA capabilities has enabled access to the molecular gas emission from quiescent galaxies through observations of dust continuum and CO line emission at $z < 3$ (e.g. Gobat et al. 2018; Whitaker et al. 2021; Williams et al. 2021). Such observations have allowed studying the evolution of these populations in the context of more active star-forming main-sequence galaxies and put into question the validity of the scaling relations for these galaxies.

[CII] emission at $z > 4$. The [CII] line has been used extensively to target the ISM in massive star-forming galaxies at high redshift. When redshifted, this line falls into the accessible atmospheric windows from the ground, making it an ideal tracer of the ISM conditions and dynamics at $z > 3$. This has been exploited by various studies (e.g., Capak et al. 2015; Smit et al. 2018; Bakx et al. 2020), and most recently by two ALMA large programs, ALPINE (Le Fèvre et al. 2020) and REBELS (Bouwens et al. 2022), targeting galaxies at $z = 4-6$ and $6.5-9$, respectively.

Archival surveys. A different approach has been to use the ALMA archival data to detect all the dusty and line-emitting sources in the extragalactic pointing observations (Liu et al. 2019). This extremely successful approach significantly increased the number of detected objects at high redshift.

https://doi.org/10.1017/S1743921322003854 Published online by Cambridge University Press

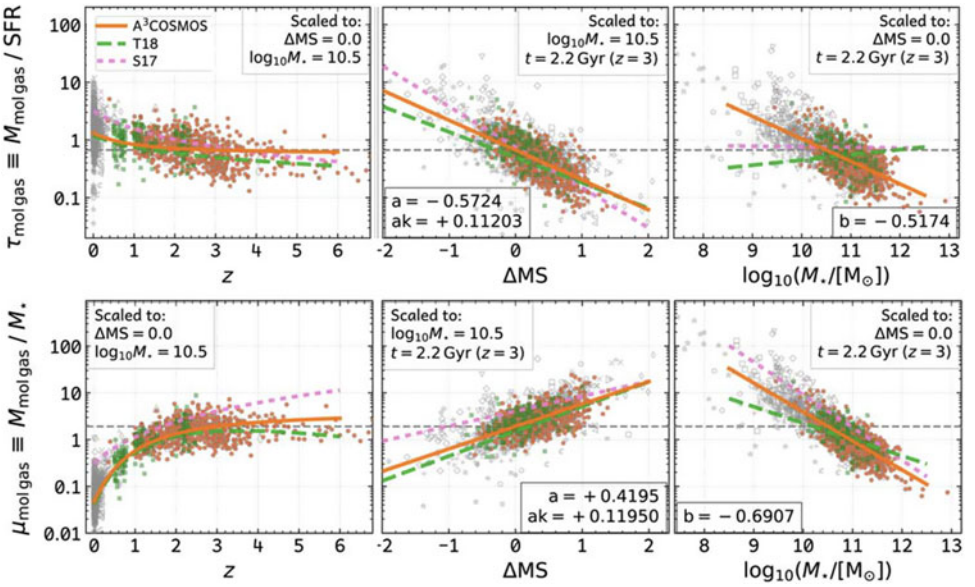

Figure 1. Scaling relations of the molecular gas to stellar mass ratio and molecular gas depletion timescale as a function of redshift, distance to the main sequence, and stellar mass (adapted from Liu et al. 2019). The molecular gas to stellar mass ratio changes by $\sim 5\times$ in the redshift range $0-2$, while the gas depletion timescale evolves only mildly. Galaxies below/above the main sequence have lower/higher gas fractions and longer depletion timescales.

3.2. *Interferometric cosmological deep fields*

Recent deep millimeter continuum surveys over increasingly large contiguous areas with ALMA toward cosmological deep fields area revolutionizing galaxy evolution studies by accessing the dust emission from the faint star-forming galaxy population.

These surveys have followed a "wedding cake" approach, covering large areas at shallower depths and narrow areas deeper and concentrating in the 1-mm band as it is more efficient in reaching good depth and area coverage (Franco et al. 2018; Hatsukade et al. 2018; Umehata et al. 2018; Dunlop et al. 2017; Hatsukade et al. 2016); and most recently two ALMA large programs, The ALMA Spectroscopic Survey in the HUDF (ASPECS; Walter et al. 2016; Gonzalez-Lopez et al. 2020) and the ALMA Lensing Cluster Survey (ALCS; Fujimoto et al. 2021). In the particular case of ASPECS, it provided a complementary approach to pure continuum millimeter-deep field observations, simultaneously observing CO/[CI] and [CII] line emission at all redshifts, along with continuum emission at 3mm and 1mm over the full Hubble Ultra Deep Field (HUDF). The availability of ancillary data has been key to providing a detailed characterization of the identified galaxies.

4. ISM evolution at high redshift

The surveys described above enabled the determination of key scaling relations between molecular gas fraction and depletion timescales, with redshift, stellar mass, and distance to the main sequence, which describes how galaxies regulate the stellar mass growth (Fig. 1; e.g. Tacconi et al. 2020).

Surveys of quiescent galaxies revealed stringent limits on gas fraction, with gas fractions $< 6\%$ for galaxies $> 3x$ below the main sequence, being still unclear the actual mechanisms for star formation quenching, whether through truncation of gas accretion

https://doi.org/10.1017/S1743921322003854 Published online by Cambridge University Press

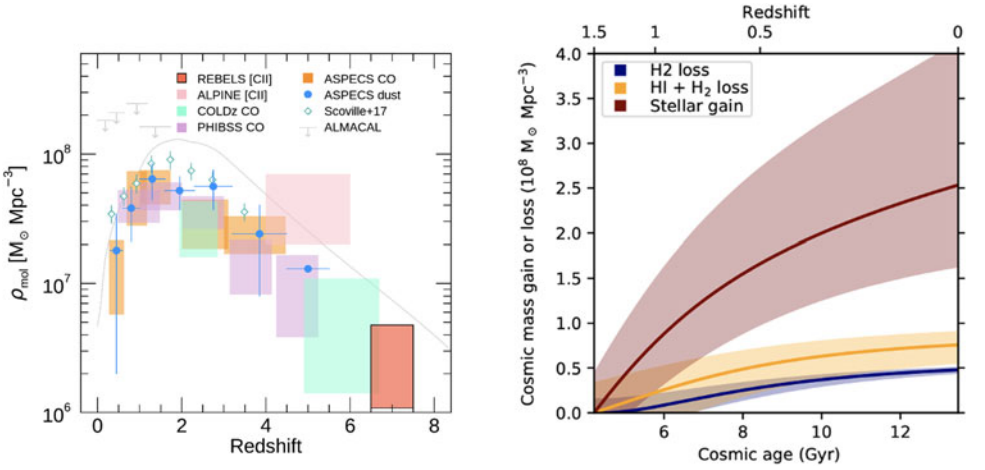

Figure 2. *(Left:)* Cosmic density of molecular gas as seen by various surveys for CO, dust, and [CII] line emission (from Aravena et al. in preparation; see also Decarli et al. 2020). The evolution of the cosmic molecular gas density appears to mimic the cosmic SFR density out to $z \sim 7$. *(Right:)* Cumulative gain of stellar mass since $z = 1.5$ to $z = 0$, compared to the loss of ISM gas, including H_2 and HI. This comparison suggests that gas accretion is needed to explain the difference between the amount of mass gained in stars and loss in gas.

truncation (gas depletion), or associated to low mass halos with strong feedback, or efficient gas consumption (Williams et al. 2021; Whitaker et al. 2021). An interesting individual example is Spilker et al. (2022), where resolved CO observations in a post-starburst galaxy at $z = 0.7$ showed the possibility of gas removal from the galaxy center through a recent merger.

Similarly, these surveys enabled the measurement of the cosmic molecular gas density (see Fig. 2). This seems to mimic the evolution of the cosmic SFR density, indicating a close link between both quantities and relatively constant efficiencies out to $z \sim 5-6$ (Decarli et al. 2020; Aravena et al. in preparation). Indeed by accounting for the contribution of the stellar, HI, and H2 cosmic mass densities, Walter et al. (2020) were able to argue that the significant gap between the number of stars created in the universe and the available gas (HI+H2) that can be used for star formation could only be explained by gas accretion from the galaxies circumgalactic medium (Fig. 2).

5. The next step? kpc-scale tomography of galaxies at high redshift

Understanding the physical processes of star formation within individual galaxies requires higher angular resolution. So far, the focus has been on the optical regime, centered on Hα and [OIII]5007 imaging at $z \sim 2$ using AO IFU and rest-UV using HST. The picture suggests that star formation occurs in massive clumps within turbulent disks (e.g. Genzel et al. 2008; Soto et al. 2017). However, such studies might be biased due to global obscuration across the sources, particularly in massive galaxies (Simpson et al. 2017; Hodge et al. 2019), based on the offsets seen between rest-UV and FIR components and the different extent and structure at the different wavelengths.

Resolved ISM observations exist only in a handful of objects. They have been mostly focused on size measurements from unresolved (Puglisi et al. 2019) and resolved continuum FIR observations (e.g. Barro et al. 2016; Tadaki et al. 2020; Chen et al. 2020; Cochrane et al. 2021). Current results indicate that the FIR emission is almost always more compact than optical and stellar mass sizes and that the central regions in galaxies can be starbursting, while outer disks are in the MS. So far, only a handful of sources

https://doi.org/10.1017/S1743921322003854 Published online by Cambridge University Press

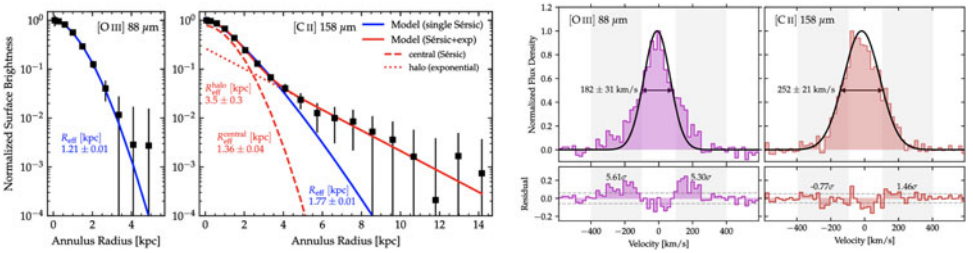

Figure 3. [OIII] 88 μ and [CII] 158μm line emission in a galaxy at $z = 7.1$ (adapted from Akins et al. 2022). *(Left:)* Comparison of the radial distribution of both lines shows that the [CII] emission is extended and can be described by a compact and an extended component. *(Right:)* The emission line profiles indicate a wider [CII] line profile, but with a double component [OIII] profile, which can be attributed to an outflow of ionized gas. Outflows have become a possibility to explain the extended [CII] structures seen recently in distant galaxies.

have resolved CO line emission observations both in unlensed (e.g. Spilker et al. 2019) and lensed objects (Dessauges-Zavadsky et al. 2019).

6. Feedback in action at high redshift?

The recent ALPINE and REBELS [CII] surveys of galaxies at $z > 4$ have found interesting results. Intriguingly, ALPINE finds evidence of extended [CII] emission, or "[CII]" halos around $z \sim 4-6$ galaxies. In particular, they find a 30-kpc scale halo in a multiple merger system at $z \sim 4$ (Ginolfi et al. 2020), while clear evidence that the [CII] radial distribution extends beyond rest-UV in massive galaxies in this redshift range both in individual cases and using stacking (Fujimoto et al. 2020). It is still unclear what the origin of the "halos" might be, with current possibilities being outflows, inflows, tidal tails, or mergers.

These surveys found key supporting evidence for the existence of rotating disks already at $z \sim 7$ (Smit et al. 2018). Similarly, ALPINE observations find that $\sim 40\%$ of galaxies at $z = 4-6$ show signs of rotating disks (Jones et al. 2020). [CII] size measurements from the REBELS and ALPINE surveys reveal little size evolution from $z \sim 4$ to 7, despite the decreasing UV-sizes at higher redshifts (Fudamoto et al. 2022a)

Resolved [CII] studies with ALMA toward a few galaxies at $z \sim 5-7$ have found contrasting results. Herrera-Camus et al. (2022) find evidence for a rotating disk and an outflow in a massive star-forming galaxy at $z = 5.5$. However, only mild evidence is found for extended [CII] emission, similar to the system studied by Posses et al. (2022) at $z = 6.8$. Akins et al. (2022) find an extended [CII] "halo" toward a galaxy at $z = 7.1$ when compared to the dust and rest-frame UV distributions and clear signatures for outflowing gas, indicating that outflows can be associated with the [CII] "halo' (Fig. 3). Finally, Lambert et al. (2022) find an extended [CII] emission compared to the rest-frame UV. However, the kinematics rather suggest a merger as the origin for the extended "halo".

Clearly, high-resolution multi-wavelength observations are needed to unveil the nature of distant galaxies and the associated build-up and feedback processes.

6.1. *The ALMA CRISTAL large program survey*

CRISTAL is a recently approved Cycle 8 ALMA Large Program (139 hr) that will spatially resolve the [CII] 158μm line and dust continuum emission in 19 mass-selected star-forming galaxies at $z \sim 4-5$ (Fig. 4). All CRISTAL galaxies have HST rest-frame UV data, and more than half of them will have Cycle 1 JWST rest-frame optical observations. With the combination of ALMA, HST, and JWST, CRISTAL will produce the

https://doi.org/10.1017/S1743921322003854 Published online by Cambridge University Press

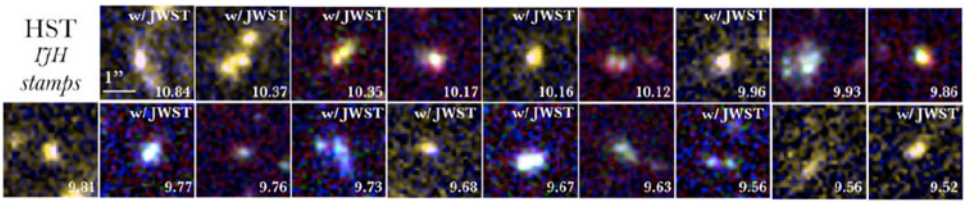

Figure 4. HST Postage stamps in the optical/NIR toward the mass-selected sample of 19 CRISTAL galaxies. Approximately half of the sample is expected to ave JWST imaging during its first 2 years of observations (Credit: R. Herrera-Camus, N. Förster-Schreiber).

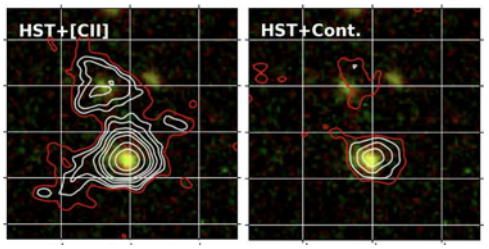

Figure 5. Example of the [CII] line and FIR continuum emission in one of the CRISTAL galaxies. The background image was created from the HST imaging, and the contours represent the [CII] line and FIR continuum emission, respectively. It is evident the difference in structure and extent seen in the ALMA and HST images.

first systematic census of gas, dust, and stars on $\sim 1-2$ kpc scales in typical star-forming galaxies when the Universe was only 1 Gyr old. This will allow us to connect the properties of the ISM, circumgalactic medium, star formation, and feedback in the form of outflows (Fig. 5).

7. Concluding remarks

• Observations of the ISM of galaxies at high redshift has provided a foundational framework for galaxy evolution and the transformation of gas to stars in galaxies. Recent studies of quiescent galaxies indicate that current scaling relations might not be valid for quenched objects.

• Measurements of the cosmic density of molecular gas indicate a simultaneous and similar evolution to that of the cosmic density of SFR. The current observations imply the need for cosmic gas accretion to match the number of stars created in the last 1.5 Gyr of cosmic time.

• Resolved observations of the ISM in high redshift galaxies are still scarce and focused mostly on the dust continuum emission. There is still debate about the mechanisms for quenching at $z < 2$.

• Recent ALMA large programs and follow-up higher resolution observations have suggested the existence of rotating disks and [CII] halos in galaxies at $z = 4-7$. The ALMA CRISTAL large program will provide insights on the origin and reality of these findings.

Acknowledgements

MA acknowledges support from FONDECYT grant 1211951, ANID+PCI+INSTITUTO MAX PLANCK DE ASTRONOMIA MPG 190030, ANID+PCI+REDES 190194 and ANID BASAL project FB210003.

https://doi.org/10.1017/S1743921322003854 Published online by Cambridge University Press

References

Aravena, M., Spilker, J. S., Bethermin, M., et al. 2016, *MNRAS*, 457, 4406
Birkin, J. E., Weiss, A., Wardlow, J. L., et al. 2021, *MNRAS*, 501, 3926
Bakx, T. J. L. C., Tamura, Y., Hashimoto, T, et al. 2020, *MNRAS*, 493, 4294
Barro, G., Kriek, M., Pérez-González, P. G., et al. 2016, *ApJ*, 827, 32
Bolatto, A., Wolfire, M., Leroy, A. et al. 2013, *ARA&A*, 51, 207
Bothwell, M. S., Smail, I., Chapman, S. C., et al. 2013, *MNRAS*, 429, 3047
Bouwens, R. J., Smit, R., Schouws, S., et al. 2022, *ApJ*, 931, 160
Capak, P. L., Carilli, C. L., Jones, G., et al. 2015, *Nature*, 522, 455
Cañameras, R., Yang, C., Nesvadba, N. P. H., et al. 2018, *A&A*, 620, 61
Casey, C. M., Narayanan, D., Cooray, A., et al. 2014, *PhR*, 541, 45
Chen, C. C., Harrison, C. M., Smail, I. et al. 2020, *A&A*, 635, 119
Cochrane, R. K., Best, P. N., Smail, I. et al. 2021, *MNRAS*, 503, 2622
Decarli, R., Aravena, M., Boogaard, L. et al. 2020, *ApJ*, 902, 110
Dessauges-Zavadsky, M., Richard, J., Combes, F. et al. 2019, *NatAs*, 3, 1115
Dunlop, J. S., McLure, R. J., Biggs, A. D. et al. 2017, *MNRAS*, 466, 861
Elbaz, D., Daddi, E., Le Borgne, D., et al. 2007, *A&A*, 468, 33
Franco, M., Elbaz, D., Béthermin, M. et al. 2018, *A&A*, 620, 152
Fudamoto, Y., Smit, R., Bowler, R. A. A. et al. 2022, *ApJ*, 934,144
Fujimoto, S., Silverman, J. D., Béthermin, M. et al. 2020, *ApJ*, 900, 1
Fujimoto, S., Oguri, M., Brammer, G. et al. 2021, *ApJ*, 911, 99
Genzel, R., Burkert, A., Bouché, N. et al. 2008, *ApJ*, 687, 59
Ginolfi, M., Jones, G. C., Bethermin, M. et al. 2020, *A&A*, 643, 7
Gobat, R., Daddi, E., Magdis, G., et al. 2018, *NatAs*, 2, 239
González-López, J., Decarli, R., Pavesi, R. et al. 2019, *ApJ* accepted, arxiv:1903.09161
Harrington, K. C., Yun, M. S., Magnelli, B. et al. 2018, *MNRAS*, 474, 3866
Heintz, K. E., Watson, D., Oesch, P. et al. 2021, *ApJ*, 922, 147
Hatsukade, B., Kohno, K., Umehata, H. et al. 2016, *PASJ*, 68, 36
Hatsukade, B., Kohno, K., Yamaguchi, Y. et al. 2018, *PASJ*, 70, 105
Herrera-Camus, R., Forster-Schreiber, N., Price, S. H. et al. 2022, *A&A*, 665, 8
Hodge, J. A., Smail, I., Walter, F., et al. 2019, *ApJ*, 876, 130
Hughes, D. H., Serjeant, S., Dunlop, J., et al. 1998, *Nature*, 394, 241
Jones, G. C., Bethermin, M., Fudamoto, Y. 2019, *MNRAS*, 491, 18
Lambert, T. S., Posses, A., Aravena, M. et al. 2022, *ArXiv:2210.10023*
Le Fèvre, O., Béthermin, M., Faisst, A., et al. 2020, *A&A*, 643, A1
Liu, D., Lang, P., Magnelli, B. et al. 2019, *ApJS*, 244, 40
Madau, P. & Dickinson, M. 2004, *ARA&A*, 52, 415
Posses, A. C., Aravena, M., González-López, J. et al. 2022, *ArXiv:2206.13770*
Sharon, C. E., Riechers, D. A., Hodge J., et al. 2016, *ApJ*, 827, 18
Scoville, N., Aussel, H., Sheth, K. et al. 2014, *ApJ*, 783, 84
Scoville, N., Lee, N., Vanden Bout, P., et al. 2015, *ApJ*, 837, 150
Simpson, J. M., Smail, I., Swinbank, A. M. et al. 2017, *ApJ*, 839, 58
Smail, I., Ivison, R. J., & Blain, A. W. 1997, *ApJL*, 490, 5
Smit, R., Bouwens, R. J., Carniani, S. et al. 2018, *Nature*, 553, 178
Soto, E., de Mello, D. F., Rafelski, M. et al. 2017, *ApJ*, 837, 6
Spilker, J. S., Bezanson, R., Weiner, B. J. et al. 2019, *ApJ*, 883, 81
Spilker, J. S., Suess, K. A., Setton, D. et al. 2022, *ApJ*, 936, 11
Tadaki, K., Belli, S., Burkert, A., et al. 2020, *ApJ*, 901, 74
Tacconi, L. J., Genzel, R., Saintonge, A., et al. 2018, *ApJ*, 853, 179
Tacconi, L. J., Genzel, R., Sternberg, A. 2020, *ARA&A*, 58, 157
Umehata, H. Hatsukade, B., Smail, I. et al. 2018, *PASJ*, 70, 65
Valentino, F., Magdis, G. E., Daddi, E. et al. 2018, *ApJ*, 869, 27
Walter, F., Decarli, R., Aravena, M. et al. 2016, *ApJ*, 833, 67
Walter, F., Carilli, C. L., Neeleman, M. et al. 2020, *ApJ*, 902, 111

Wardlow, J. L., Simpson, J. M., Smail, I. et al. 2018, *MNRAS*, 479, 3879
Whitaker, K. E.., Williams, C. C., Mowla, L. et al. 2021, *Nature*, 579, 485
Williams, C. C., Spilker, J., Whitaker, K. E. et al. 2021, *ApJ*, 908, 54
Yang, C., Omont, A., Beelen, A. et al. 2017, *A&A*, 608, 144
Zanella, A., Daddi, E., Magdis, G. et al. 2018, *MNRAS*, 481, 2

https://doi.org/10.1017/S1743921322003854 Published online by Cambridge University Press